Cloud-Free Imaging Probability Forecasting for Optical Earth-Observation Tasking over Yerevan, Armenia

Isabella Avasapian
Teevial
info@teevial.org

July 14, 2026

Abstract

Optical Earth-observation satellites such as Sentinel-2 cannot see through cloud, so a tasking attempt over a cloudy target wastes a limited imaging window along with onboard power and downlink bandwidth. We study whether next-day cloud conditions over Yerevan, Armenia can be forecast accurately enough to automate the binary Go/No-Go tasking decision. Daily cloud-free fractions are derived from the Sentinel-2 Level-2A scene classification for 933 days spanning 2020–2024 and paired with ten ERA5 atmospheric reanalysis variables; four days of atmospheric context (today and three lags) form a 40-feature predictor for the following day's cloud-free fraction. Using strictly time-ordered cross-validation, a gradient-boosted tree model (XGBoost) attains a mean absolute error of 0.165 on the cloud-free fraction and a random forest attains 0.160, improving on a persistence baseline (0.169) by 2.4–5.5%. Because cloudiness over the orographically stable Ararat Valley is strongly autocorrelated, persistence is a demanding benchmark, and the learned gain reflects a genuine atmospheric signal rather than trend-following. An operational variant generalizes the approach to multiple Armenian regions, is calibrated as a probabilistic Go/No-Go classifier (cross-validated AUC 0.77, Brier score 0.17 over 5,736 samples), and is driven at inference time by the cloud-free, no-key Open-Meteo forecast API to sidestep the production latency of ERA5. We release the system as an openly accessible high-frequency cloud-imaging forecast for the South Caucasus, a tool that to our knowledge does not otherwise exist for the region.

1 Introduction

Optical sensors aboard satellites such as the European Space Agency's Sentinel-2 constellation image the Earth in visible and near-infrared bands [4]. Clouds are opaque at these wavelengths, so any scene acquired through cloud is partially or wholly unusable for downstream analysis such as change detection, land-use classification, or infrastructure monitoring. Tasking a satellite to image a specific target consumes a scheduled pass, onboard power, and downlink bandwidth; when the acquisition is spoiled by cloud, those resources are lost and the next opportunity may be days away given the constellation's revisit cycle. A reliable next-day forecast of cloud conditions over a target therefore has direct operational value: it converts a blind acquisition into an informed *Go/No-Go* decision.

This paper develops such a forecast for Yerevan, the capital of Armenia and the country's highest-value optical-imaging target. Yerevan sits in the Ararat Valley at roughly 1,000 m elevation, one of the lowest-cloud-cover regions of the South Caucasus, where orographically stable weather produces strong day-to-day persistence that a lag-based model can exploit. We pose the problem as next-day regression of a *cloud-free fraction*, the share of a target area unobstructed by cloud, and threshold the prediction to recover the operational binary decision.

Contributions.

1. We construct a five-year daily dataset for Yerevan that pairs Sentinel-2 Level-2A cloud-free labels with ERA5 atmospheric reanalysis, using an efficient label source that avoids downloading raw imagery tiles (Section 3).
2. We formalize the tasking problem as next-day cloud-free-fraction regression with an atmospheric-persistence feature design, and evaluate three models under strictly time-ordered cross-validation against a persistence baseline (Sections 4–5).
3. We deploy an operational, multi-region probabilistic variant driven by a public forecast API, and release it as an openly accessible cloud-imaging forecast for the South Caucasus, a resource that, to our knowledge, is otherwise absent for the region.

2 Related Work

Short-range cloud prediction sits between numerical weather prediction (NWP) and statistical learning. Operational NWP systems and reanalyses such as ERA5 [6] assimilate heterogeneous observations into physically constrained atmospheric states and are the gold standard for retrospective analysis, but their production latency makes the most recent days unavailable for real-time inference. A complementary line of work treats cloud and irradiance prediction as a supervised learning problem over engineered atmospheric features, where gradient-boosted decision trees [3, 8] and random forests [2] are competitive and robust on tabular, modestly sized datasets. For time-ordered data, naive random cross-validation leaks future information into training and inflates reported skill; time-aware evaluation is required for credible estimates [1, 7]. Persistence, that is, predicting that tomorrow equals today, is the standard reference baseline in meteorological forecasting and is notoriously hard to beat in autocorrelated regimes. Our work applies these principles to a concrete satellite-tasking decision, emphasizes an honest persistence comparison, and adds model interpretability through gain-based importances and Shapley attribution [9].

3 Study Area and Data

3.1 Area of interest

The target is a 35×22 km bounding box over Yerevan. A city-scale area of interest yields a sharper, more operationally meaningful forecast than a country-wide average, because a tasking decision always concerns a specific scene. Critically, 81.8% of labeled days in the historical record exceed the 70% cloud-free imaging threshold defined below: Yerevan is a clear-sky-dominant location, and the central modeling challenge is to correctly flag the roughly one-in-five days that fall below threshold.

Table 1: ERA5 single-level predictors, spatially averaged over the Yerevan area of interest.

Variable	Quantity	Relevance
`tcc`	Total cloud cover	Direct cloud state; strongest single predictor
`lcc`	Low cloud cover	Stratus and fog; most opaque to optical sensors
`mcc`	Medium cloud cover	Mid-level cloud
`hcc`	High cloud cover	Cirrus; thinner and less obstructive
`tcwv`	Total column water vapour	Cloud-formation potential
`msl`	Mean sea-level pressure	High pressure favours subsidence and clear skies
`t2m`	2 m temperature	Thermal stratification; season proxy
`d2m`	2 m dewpoint temperature	Dewpoint spread indicates atmospheric dryness
`u10`, `v10`	10 m wind components	Advection of air masses

3.2 Sentinel-2 cloud-free labels

The Sentinel-2 mission provides a 2–5 day revisit with two polar-orbiting satellites; the atmospherically corrected Level-2A product carries a Scene Classification Layer (SCL) generated by the Sen2Cor processor, which labels each pixel by surface or cloud type [10]. Deriving labels from full SCL rasters would require downloading 0.5–1 GB per scene, of order 500–900 GB across five years. Instead we retrieve the scene-level `cloudCover` attribute exposed by the Copernicus Data Space OData service [5], which Sen2Cor computes directly from the SCL during Level-2A production and is therefore the SCL-derived cloud-free fraction pre-aggregated by the agency. The daily label is

$$\mathrm{cf} \;=\; \frac{100 - \texttt{cloudCover}}{100} \;\in\; [0, 1], \tag{1}$$

and where several scenes exist for one day the clearest (lowest `cloudCover`) is retained, giving one label per day. Querying the L2A collection intersecting the Yerevan box over 2020-01-01 to 2024-12-31, with year-by-year pagination to respect the API's record-skip limit, yields 933 unique labeled days.

3.3 ERA5 atmospheric predictors

Predictors are drawn from ERA5 [6], the fifth-generation ECMWF global reanalysis at $\sim$31 km resolution. Ten single-level variables (Table 1) are spatially averaged over the Yerevan box to one value per day at the 12:00 UTC snapshot.

4 Methodology

4.1 Feature design: atmospheric persistence

The governing intuition is that cloud conditions are strongly autocorrelated from one day to the next: a high-pressure system over the Ararat Valley does not dissipate overnight, and cloudy regimes likewise persist. Each prediction is therefore conditioned on four consecutive days of ERA5 context: the current day T and lags $T-1$, $T-2$, $T-3$. With ten variables per day this yields a 40-dimensional feature vector, and the regression target is the Sentinel-2 cloud-free fraction on day $T+1$. Each training row thus answers: *given the weather over Yerevan across the last four days, how cloud-free will tomorrow be?*

Table 2: Expanding-window time-series cross-validation folds (row indices into the chronologically ordered dataset).

Fold	Training rows	Test rows	Approx. test period
1	1–154	155–309	2020
2	1–309	310–464	2020–2021
3	1–464	465–619	2021–2022
4	1–619	620–774	2022–2023
5	1–774	775–929	2023–2024

4.2 Models

We evaluate three approaches:

- **XGBoost** [3]: gradient-boosted regression trees (300 trees, maximum depth 4, learning rate 0.05, subsample 0.8) predicting the cloud-free fraction as a continuous value in $[0, 1]$; the deployed single-AOI model.
- **Random forest** [2]: a bagged-tree ensemble (200 trees, maximum depth 6) used as a comparison.
- **Persistence baseline**: the no-learning reference that predicts tomorrow equals today, essential for judging whether either model adds real value.

Models are implemented with scikit-learn and the XGBoost library [3, 11].

4.3 Time-ordered evaluation

Because the data are a time series, ordinary random cross-validation would train on future days and test on past ones, producing optimistic and meaningless skill estimates [1]. We use an expanding-window scheme (`TimeSeriesSplit`, five folds) in which each fold's test set lies strictly after its training set in time (Table 2); the training window grows by one block per fold. Skill is summarized by the mean absolute error (MAE) on the cloud-free fraction, averaged across folds with its standard deviation.

4.4 Decision rule

For tasking we threshold the predicted cloud-free fraction $\widehat{\mathrm{cf}}$ at $\tau = 0.70$:

$$\text{decision} = \begin{cases} \textsc{Go} & \widehat{\mathrm{cf}} \geq \tau, \\ \textsc{No-Go} & \widehat{\mathrm{cf}} < \tau. \end{cases} \tag{2}$$

Below 70% cloud-free, obstruction degrades optical image quality for most analytical uses. Historically 81.8% of days satisfy the Go condition and 18.2% do not.

4.5 Operational live system

ERA5 has a production latency of roughly five days and so cannot drive a genuine next-day forecast. At inference time the operational system instead queries Open-Meteo, a free, no-key, ECMWF-based forecast service [12]: it retrieves the past four days plus the current day over the Yerevan area,

Table 3: Cross-validated mean absolute error (MAE) on the cloud-free fraction, five-fold time-series cross-validation. Lower is better.

Model	CV MAE ± std	vs. baseline
Persistence baseline	0.1694 ± 0.0217	n/a
XGBoost (deployed)	0.1653 ± 0.0148	−2.4%
Random forest	$\mathbf{0.1601 \pm 0.0163}$	−5.5%

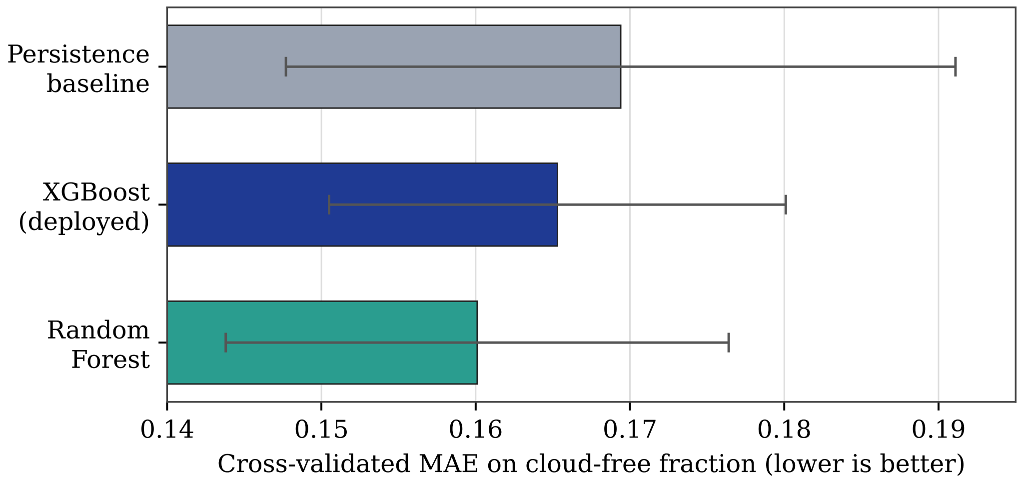

Figure 1: Cross-validated MAE on the cloud-free fraction for the persistence baseline, XGBoost, and random forest. Error bars show ± one standard deviation across the five time-series folds.

converts units to the ERA5 convention (percentages to fractions, hPa to Pa, °C to K, wind speed and direction to u/v components), substitutes a monthly climatological mean for total column water vapour where the forecast field is unavailable, assembles the feature vector in the exact training column order, and applies the saved model to emit the Go/No-Go recommendation. The public-facing dashboard refreshes from this same source.

5 Results

5.1 Forecast accuracy against persistence

Table 3 and Figure 1 report cross-validated MAE for the Yerevan study. XGBoost improves on persistence by 2.4% and the random forest by 5.5%. The improvements are modest in absolute terms, which is expected: cloud cover over the Ararat Valley is highly autocorrelated, making persistence a strong heuristic, so any gain over it represents a learned atmospheric signal rather than mere trend-following. That the random forest slightly outperforms the gradient-boosted model is a common outcome on small datasets, where boosting benefits less from its added capacity; XGBoost was retained as the deployed model per the original design, but the difference is noted.

In operational terms a 2–5% reduction in wasted acquisitions compounds over a year: at, say, 200 tasking attempts over Yerevan annually, a 2.4% improvement recovers on the order of five additional successful imaging days, ground coverage that would otherwise be lost to cloud.

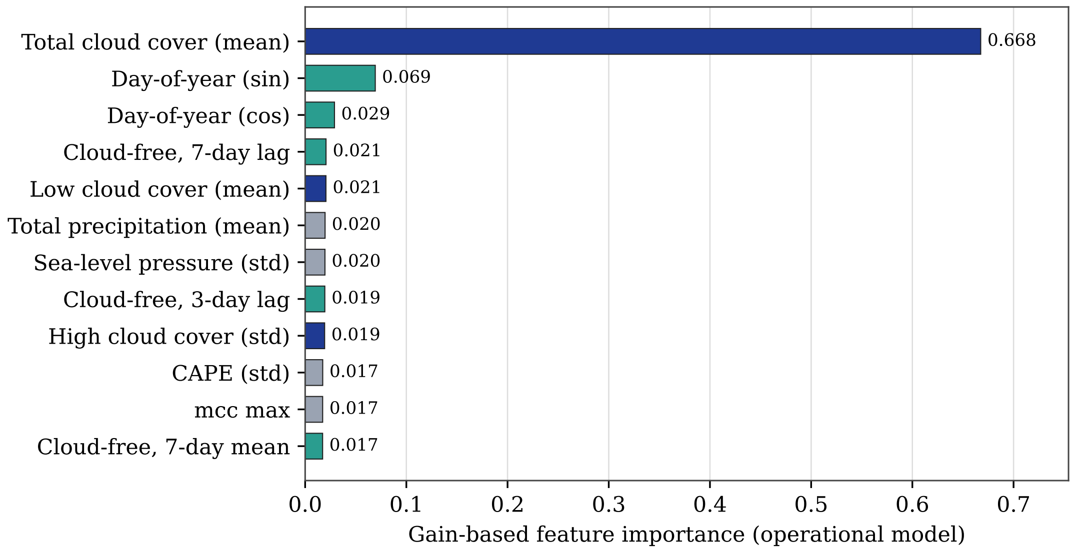

Figure 2: Top twelve gain-based feature importances of the operational model. Cloud-cover aggregates (dark) dominate; cyclical day-of-year seasonality and observed cloud-free persistence lags (teal) account for most of the remaining weight.

5.2 What the model attends to

Figure 2 shows the gain-based feature importances of the operational multi-region model (Section 5.4). Total cloud cover and its aggregate statistics dominate, which is meteorologically sensible: the present cloud state is the strongest available signal for the near term. Below it, two interpretable families carry most of the remaining weight: seasonality, encoded as cyclical day-of-year terms, and persistence, encoded as multi-day lags and rolling statistics of the observed cloud-free fraction. The prominence of the lag and seasonal features confirms the atmospheric-persistence hypothesis that motivated the feature design. Gain-based rankings agree with the qualitative direction of Shapley attribution [9] computed on the same model.

5.3 Seasonal structure

Yerevan's continental semi-arid climate imposes a strong seasonal signal on imaging reliability (Figure 3). Summer (June–August) is the prime window at 90–98% cloud-free under continental high pressure; early autumn (September–October) remains reliable at 86–89%; the winter cloud season (November–March) falls to 42–55%, where below-threshold risk is substantial; and spring (April–May) recovers through 62–76%. The forecast is most valuable in the shoulder seasons, where day-to-day variability is greatest and naive persistence performs worst.

5.4 Operational deployment

Beyond the Yerevan study, an operational variant generalizes the method to multiple Armenian areas of interest and is trained as a calibrated probabilistic Go/No-Go classifier alongside the fraction regressor. Trained on 5,736 daily samples with 59 features (the ten ERA5 fields and their multi-day aggregates, total precipitation and convective available potential energy, cyclical seasonality terms, observed cloud-free persistence lags, and per-AOI geographic identifiers), it attains a cross-validated

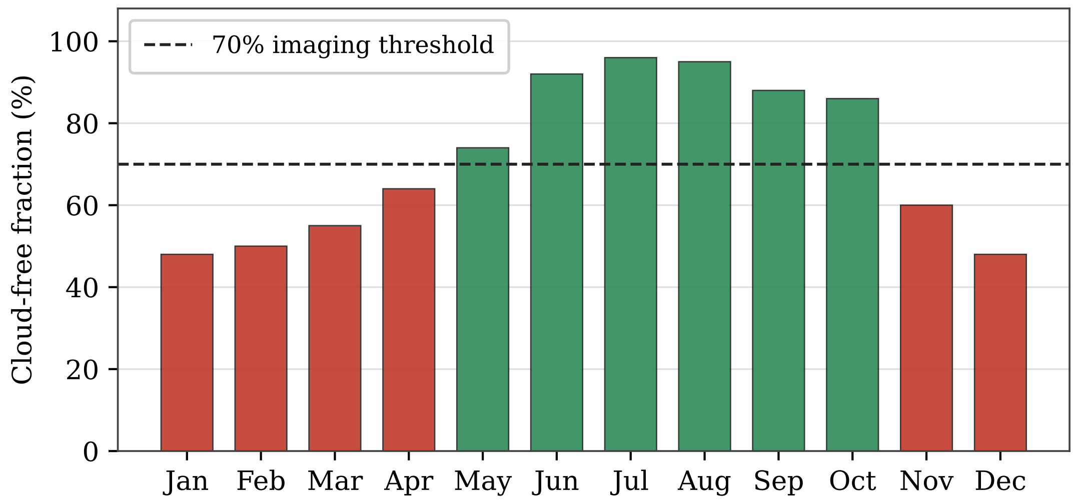

Figure 3: Representative monthly cloud-free fraction over Yerevan (Sentinel-2, 2020–2024). The dashed line marks the 70% imaging threshold; months below it (red) carry elevated No-Go risk.

Table 4: Operational multi-region model, time-series cross-validated.

Metric	Value
Training samples	5,736
Features	59
Decision threshold	0.70
Cross-validated ROC-AUC	0.770
Brier score	0.174
Regression MAE	0.152
Regression RMSE	0.187

ROC-AUC of 0.77 and a Brier score of 0.17 for the binary threshold decision, with a regression MAE of 0.15 (Table 4). The probabilistic output is the operationally meaningful quantity near the decision boundary, where a binary verdict is most sensitive to small errors in the predicted fraction.

6 Discussion

The results support a deliberately modest but operationally useful claim. In a clear-sky-dominant, orographically stable basin, the dominant predictor of tomorrow's cloud state is today's, and a well-tuned tree ensemble extracts only a few percentage points of additional skill over persistence. Yet in a tasking context those points are not noise: each avoided cloudy acquisition is a recovered imaging opportunity, and the value concentrates exactly where it is needed: the volatile shoulder seasons and the minority of below-threshold days that a persistence rule handles worst. Framing the output as a calibrated probability, rather than a hard label, lets an operator trade off missed opportunities against wasted passes according to mission priorities instead of accepting a fixed threshold.

7 Limitations

Several limitations bound the present results. (i) Labels use ESA's scene-level `cloudCover` attribute rather than pixel-level SCL statistics clipped exactly to the AOI polygon; the two are mathematically consistent, but pixel-level processing would give a more precise boundary fraction. (ii) Training uses ERA5 while live inference uses Open-Meteo, introducing a potential domain shift near the decision threshold, and total column water vapour is approximated by a climatological mean in the live path. (iii) The single-AOI dataset of 929 usable rows is small for machine learning; ERA5 extends to 1940 and a longer record would likely improve generalization. (iv) The models emit point estimates in the single-AOI study; a calibrated interval, available in the operational classifier, is most important near the 70% threshold. (v) Forecasts are single-step ($T{+}1$); multi-day horizons would require recursive prediction or dedicated retraining.

8 Conclusion and Future Work

We presented a next-day cloud-free imaging forecast for optical satellite tasking over Yerevan, built from five years of Sentinel-2 labels and ERA5 reanalysis, evaluated honestly against a strong persistence baseline under time-ordered cross-validation, and deployed as an openly accessible, multi-region probabilistic Go/No-Go service driven by a public forecast API. Natural extensions include pixel-level SCL processing via the SentinelHub Statistical API for exact AOI fractions; driving inference directly from ECMWF medium-range forecasts to remove the reanalysis-to-forecast domain shift; multi-day forecast horizons; season-specific models for Yerevan's distinct wet winter and dry summer; explicit uncertainty quantification; and additional areas of interest across Armenia such as Gyumri, Lake Sevan, and the Lori highlands, enabling regional comparison of imaging windows.

Data and Code Availability

Sentinel-2 imagery is distributed by the Copernicus Data Space Ecosystem [5]; ERA5 is distributed by the Copernicus Climate Change Service [6]; live forecasts use the Open-Meteo API [12]. A reproducibility package accompanies this paper, containing the area-of-interest definitions, the 59-feature engineering layer, the gradient-boosted model with time-ordered cross-validation, the documented Sentinel-2/ERA5 data sources, and runnable scripts for both the full training pipeline and the live Open-Meteo forecast. Because the underlying Sentinel-2 and ERA5 records require credentialed downloads, the package also provides a deterministic synthetic generator that exercises the identical code path end-to-end without API keys. The code is released under the MIT license; it, together with the public dashboard, is maintained by Teevial.

References

[1] Christoph Bergmeir and José M. Benítez. On the use of cross-validation for time series predictor evaluation. *Information Sciences*, 191:192–213, 2012. doi: 10.1016/j.ins.2011.12.028.

[2] Leo Breiman. Random forests. *Machine Learning*, 45(1):5–32, 2001. doi: 10.1023/A:1010933404324.

[3] Tianqi Chen and Carlos Guestrin. XGBoost: A scalable tree boosting system. In *Proceedings of the 22nd ACM SIGKDD International Conference on Knowledge Discovery and Data Mining*, pages 785–794, 2016. doi: 10.1145/2939672.2939785.

[4] M. Drusch, U. Del Bello, S. Carlier, O. Colin, V. Fernandez, F. Gascon, B. Hoersch, C. Isola, P. Laberinti, P. Martimort, A. Meygret, F. Spoto, O. Sy, F. Marchese, and P. Bargellini. Sentinel-2: ESA's optical high-resolution mission for GMES operational services. *Remote Sensing of Environment*, 120: 25–36, 2012. doi: 10.1016/j.rse.2011.11.026.

[5] European Space Agency. Copernicus data space ecosystem. https://dataspace.copernicus.eu, 2023. Accessed 2026.

[6] Hans Hersbach, Bill Bell, Paul Berrisford, Shoji Hirahara, András Horányi, Joaquín Muñoz-Sabater, Julien Nicolas, Carole Peubey, Raluca Radu, Dinand Schepers, et al. The ERA5 global reanalysis. *Quarterly Journal of the Royal Meteorological Society*, 146(730):1999–2049, 2020. doi: 10.1002/qj.3803.

[7] Rob J. Hyndman and George Athanasopoulos. *Forecasting: Principles and Practice*. OTexts, Melbourne, Australia, 3rd edition, 2021.

[8] Guolin Ke, Qi Meng, Thomas Finley, Taifeng Wang, Wei Chen, Weidong Ma, Qiwei Ye, and Tie-Yan Liu. LightGBM: A highly efficient gradient boosting decision tree. In *Advances in Neural Information Processing Systems*, volume 30, pages 3146–3154, 2017.

[9] Scott M. Lundberg and Su-In Lee. A unified approach to interpreting model predictions. In *Advances in Neural Information Processing Systems*, volume 30, pages 4765–4774, 2017.

[10] Magdalena Main-Knorn, Bringfried Pflug, Jerome Louis, Vincent Debaecker, Uwe Müller-Wilm, and Ferran Gascon. Sen2Cor for Sentinel-2. In *Image and Signal Processing for Remote Sensing XXIII*, volume 10427, pages 37–48. SPIE, 2017. doi: 10.1117/12.2278218.

[11] Fabian Pedregosa, Gaël Varoquaux, Alexandre Gramfort, Vincent Michel, Bertrand Thirion, Olivier Grisel, Mathieu Blondel, Peter Prettenhofer, Ron Weiss, Vincent Dubourg, et al. Scikit-learn: Machine learning in Python. *Journal of Machine Learning Research*, 12:2825–2830, 2011.

[12] Patrick Zippenfenig. Open-Meteo.com weather API. Zenodo, 2023.